Am J Physiol Heart Circ Physiol 287: H1813–H1820, 2004.
First published June 17, 2004; 10.1152/ajpheart.00036.2004.

In vivo TNF-α inhibition ameliorates cardiac mitochondrial dysfunction, oxidative stress, and apoptosis in experimental heart failure

Gordon W. Moe,[1] Jose Marin-Garcia,[2] Andrea Konig,[1] Michael Goldenthal,[2] Xiangru Lu,[3] and Qingping Feng[3]

[1]*Terrence Donnelly Heart Program, St. Michael's Hospital, University of Toronto, Toronto, Ontario, Canada M5B 1W8;* [2]*The Molecular Cardiology Institute, Highland Park, New Jersey 08903; and* [3]*Departments of Medicine, Physiology and Pharmacology, University of Western Ontario, London, Ontario, Canada NGA 4G5*

Submitted 13 January 2004; accepted in final form 13 June 2004

Moe, Gordon W., Jose Marin-Garcia, Andrea Konig, Michael Goldenthal, Xiangru Lu, and Qingping Feng. In vivo TNF-α inhibition ameliorates cardiac mitochondrial dysfunction, oxidative stress, and apoptosis in experimental heart failure. *Am J Physiol Heart Circ Physiol* 287: H1813–H1820, 2004. First published June 17, 2004; 10.1152/ajpheart.00036.2004.—Heart failure is associated with increased myocardial expression of TNF-α. However, the role of TNF-α in the development of heart failure is not fully understood. In the present study, we investigated the contribution of TNF-α to myocardial mitochondrial dysfunction, oxidative stress, and apoptosis in a unique dog model of heart failure characterized by an activation of all of these pathological processes. Male mongrel dogs were randomly assigned ($n = 10$ each) to *1*) normal controls; *2*) chronic pacing (250 beats/min for 4 wk) with concomitant administration of etanercept, a soluble p75 TNF receptor fusion protein, 0.5 mg/kg subcutaneously twice weekly; *3*) chronic pacing with administration of saline vehicle. Mitochondrial function was assessed by left ventricular (LV) tissue mitochondrial respiratory enzyme activities. Oxidative stress was assessed with aldehyde levels, and apoptosis was quantified by photometric enzyme immunoassay for cytoplasmic histone-associated DNA fragments and terminal deoxynucleotide transferase-mediated nick-end labeling (TUNEL) assays. LV activity levels of mitochondrial respiratory chain enzyme complex III and V were reduced in the saline-treated dogs and restored either partially (complex III) or completely (complex V) in the etanercept-treated dogs. Aldehyde levels, DNA fragments, and TUNEL-positive cells were increased in the saline-treated dogs and normalized in etanercept-treated dogs. These changes were accompanied by an attenuation of LV dilatation and partial restoration of ejection fraction. Our data demonstrate that TNF-α contributes to progressive LV dysfunction in pacing-induced heart failure, mediated in part by a local impairment in mitochondrial function and increase in oxidative stress and myocyte apoptosis.

cytokines; cardiomyopathy; etanercept

ONE OF THE HALLMARKS of congestive heart failure (CHF) is the relentless progressive clinical course. Left ventricular (LV) remodeling is now recognized to be a crucial process mediating the progression of CHF (8). The proinflammatory cytokines, especially TNF-α, have been causally linked to LV remodeling and progression of CHF (2, 20). However, the underlying mechanisms for the link between the activation of TNF-α and the progression of CHF are unclear.

Impaired myocardial mitochondrial dysfunction, increased myocardial oxidative stress, and myocyte apoptosis have been implicated as contributors to the progression of CHF (5, 27, 43). In vitro observations have associated TNF-α with mitochondrial dysfunction, increased oxidative stress, and apoptosis. In cultured cardiac myocytes, TNF-α increases the production of reactive oxygen species (33), accompanied by mitochondrial dysfunction as manifested by reduced mitochondrial electron transport complex III activity and mitochondrial DNA damage (40). Furthermore, TNF-α also induces apoptosis in the cardiomyocytes through a variety of cellular mechanisms (19, 29, 39). However, it is unclear to what extent these in vitro effects are operative in vivo in LV remodeling and the progression of CHF.

Chronic rapid pacing in the dog induces a heart failure phenotype that closely mimics that of human dilated cardiomyopathy (30). One unique feature of this CHF model is a consistent lack of whole organ LV hypertrophy and the severe CHF induced by pacing is accompanied by impaired mitochondrial function, increased oxidative stress, and myocyte apoptosis, and accompanied by an increase in levels of immunoreactive TNF-α in the serum as well as in the LV myocardium (27, 28, 32). Furthermore, with the use of this canine model, we (4) have recently reported marked attenuation of LV remodeling and improvement in LV systolic function by in vivo inhibition of the actions of TNF-α using etanercept, a soluble p75 TNF receptor fusion protein (TNFR:Fc). Although the recently reported results of the Randomized Etanercept Worldwide Evaluation and Anti-TNF Therapy Against CHF studies have suggested no benefit from anti-TNF-α therapy in patients with CHF (6), these studies involved patients with varying degree of severity of CHF and with concomitant therapy for CHF. Many of the patients had co-morbid conditions, such as diabetes, hypertension, and coronary artery disease, thereby precluding any conclusion of the significance of TNF-α in CHF due to dilated cardiomyopathy. Accordingly, the principal aim of the current study was to test the hypothesis that TNF-α contributed to the progression of CHF in vivo via the induction of mitochondrial dysfunction, oxidative stress, and apoptosis, by studying the effects of in vivo inhibition of TNF-α using TNFR:Fc in pacing-induced CHF, a canine model of dilated cardiomyopathy.

METHODS

Animals and study design. The study population consisted of three groups of dogs (20–34 kg). Ten normal mongrel dogs served as controls. A second group of 10 mongrel dogs underwent rapid right

Address for reprint requests and other correspondence: G. W. Moe, St. Michael's Hospital, 30 Bond St., Toronto, Ontario, Canada M5B 1W8 (E-mail: moeg@smh.toronto.on.ca).

The costs of publication of this article were defrayed in part by the payment of page charges. The article must therefore be hereby marked "*advertisement*" in accordance with 18 U.S.C. Section 1734 solely to indicate this fact.

ventricular pacing (250 beats/min) for 28 days to induce severe CHF, with concomitant administration of a recombinant soluble p75 TNF-α receptor fusion protein etanercept (Amgen; Thousand Oaks, CA), at a dose of 0.5 mg/kg injected subcutaneously twice a week beginning at *day 3* of pacing. A third group of 10 mongrel dogs underwent the same pacing protocol for 3 wk with concomitant administration of the saline vehicle. The dosage and frequency of administration of etanercept was based on previous human studies (9, 41, 42), as well as our pilot pharmacokinetic studies on normal dogs, which demonstrated sustained increased plasma level of TNFR:Fc at >72 h after a single-dose administration in the absence of any hemodynamic effects (4). In addition, we (4) have recently reported that the same administration protocol of etanercept significantly attenuated LV remodeling and improved LV ejection in the paced dogs. Approval was obtained from the institutional animal research committee and the study was performed in accordance with the guidelines on the Care and Use of Experimental Animals issued by the Canadian Council on Animal Care, Ottawa, Ontario, Canada.

Induction of heart failure and in vivo studies. The method of induction of CHF by rapid pacing has been described in detail previously (30, 31). In brief, under isoflurane anesthesia, a unipolar pacemaker lead was placed in the right ventricular apex under fluoroscopic visualization through the external jugular vein, and a programmable pulse generator (Prevail 8084, Medtronic; Mississauga, Ontario, Canada) was inserted into a subcutaneous cervical pocket. The animals were allowed to recover for at least 7 days before randomization to study groups and the acquisition of baseline measurements. After baseline hemodynamic and echocardiographic measurements to ensure healthy parameters were obtained, in the paced groups, the pacer was activated to deliver impulse continuously (250 beats/min) for 4 wk to induce severe CHF. Hemodynamics measurements were obtained at baseline and again at 4 wk (terminal study), using a high-fidelity catheter introduced via the femoral artery and a thermodilution catheter introduced via the femoral vein using lidocaine anesthesia. Two-dimensional echocardiography was performed at baseline weekly to monitor changes in LV ejection fraction for safety purpose and at 4 wk. In the paced animals, the terminal hemodynamic and echocardiographic measurements were obtained with the pacemakers deactivated to allow for restoration of sinus rhythm for at least 20 min before data acquisition. Two-dimensional and M-mode echocardiographic studies (SONOS 1000, 3.5-mHz transducer; Hewlett-Packard; Bothell, WA) were used to image the LV from a right parasternal approach. The two-dimensional parasternal long-axis view of the LV was first recorded to precisely define the LV long-axis and papillary muscles. A perpendicular view with respect to the LV long axis was then obtained to obtain the two-dimensional parasternal short-axis view. Echocardiographic measures of LV remodeling and function were calculated at end diastole using the formula for a hemispheric cylinder (18, 44). With the use of the short- and long-axis dimension, LV end-diastolic volume, mass, wall thickness, and globularity were computed.

Myocardial sampling. At the conclusion of the terminal hemodynamic and echocardiographic studies, the dogs were euthanized for the sampling of LV myocardium. With the dog under a surgical plane of thiopental anesthesia, the heart was arrested with KCl and quickly extirpated and placed in cold saline. The great vessels, atria, and right ventricle were carefully trimmed away. The lateral LV free wall was excised and cut into 500-mg samples, and biopsies were taken from the skeletal muscle vastus lateralis, snap-frozen in liquid nitrogen, and stored in −80°C until assessment for subsequent analysis of tissue parameters as described in the following sections.

Myocardial and plasma TNF-α. To complement our previous observations of increased level of immunoreactive TNF-α in both the serum and LV tissue in this model (27, 28, 32), myocardial immunohistochemical staining of TNF-α was performed in control normal dogs and untreated paced dogs. Cryostat sections of LV myocardium (10 μm) were prepared, air dried, and fixed in cold acetone (−20°C) for 10 min. The endogenous peroxidase activity was blocked by 0.3% hydrogen peroxide and incubated with 10% normal mouse/goat serum. Reaction with primary antibody was then performed overnight at 4°C. After being washed in PBS, secondary antibody, IgG-peroxidase conjugated goat anti-mouse polyclonal antibody (PharmMingen; San Diego, CA) for TNF was used. Bound antibodies were detected with streptavidin-peroxidase complex using diaminobenzidine. Negative control sections were incubated with secondary antibody alone (36). Plasma TNF-α levels were determined with the use of ELISA, as in our previous reports (27, 28, 32).

Mitochondrial function. Tissues were analyzed for mitochondrial enzyme activities using tissue homogenates prepared in a buffer composed of 0.25 M mannitol, 20 mM Tris-SO_4, and 1 mM EDTA, pH 7.4, with a glass homogenizer (26). Complex I activity measured by the oxidation of NADH by ubiquinone-1 at 340 nm, complex II measured by the oxidation of succinate by ubiquinone-2 at 600 nm, complex III assayed by reduction of cytochrome *c* by ubiquinol-2 at 550 nm, complex IV assayed by oxidation of dithionite-reduced cytochrome *c* at 550 nm, complex V assayed by NADH oxidation using the coupled enzyme assay with pyruvate kinase and lactate dehydrogenase at 340 nm, and citrate synthase (CS) assayed at 412 nm were each assessed at room temperature spectrophotometrically. Assays for complexes I, III, and V were done in the presence and absence of the specific inhibitors, rotenone, antimycin A, and oligomycin, respectively, to evaluate the contribution of contaminant activities. Complex I–V activities were also expressed as activity ratios, normalized with respect to CS activity (an enzyme often used as a gauge of overall mitochondrial content). In all cases, duplicate assays were performed. Protein determination was performed according to Bradford (3).

Oxidative stress. Central to free-radical-induced cell damage is lipid peroxidation, which generates stable saturated and unsaturated aldehydes (25). To comprehensively assess oxidative stress, a complete panel of aldehydes was therefore measured from the LV myocardium with the use of a gas chromatography and mass spectroscopy method that has been described previously (12, 23, 25).

Apoptosis. To precisely characterize apoptotic cell death, apoptosis was measured by two separate methods: terminal deoxynucleotide transferase-mediated nick-end labeling (TUNEL) assay and enzyme immunoassay for cytoplasmic histone-associated DNA fragments. The in situ TUNEL assay was performed using an (Roche Biochemical; Mannheim, Germany) according to the method we previously described (32, 39). Cells were counterstained with Hoechst 33258. Apoptosis in cardiomyocytes was quantified by the number of apoptotic nuclei in the total nuclei in 50 continuous microscopic fields under ×500 magnifications by using the following formula: percent apoptosis = (apoptotic nuclei/total nuclei) × 100. The inter- and intraobserver variances of apoptosis quantification were 3.7 and 2.5%, respectively. Cardiac myocytes were identified by cell morphology and cardiac-specific troponin I staining (32, 39).

For quantitative determination of apoptosis, cytoplasmic histone-associated DNA fragments (mono- and oligonucleotides) were measured using a photometric enzyme immunoassay (cell death detection ELISA, Roche Biochemical) according the manufacturer's instructions (39). Briefly, myocardial tissue was lysed and the supernatant (cytoplasmic fraction) was obtained by centrifugation at 20,000 *g* for 10 min at 48°C. The supernatant (20 μg protein) in duplicate was added to the microtiter plate coated with anti-histone antibody and incubated for 90 min. The samples were washed, and anti-DNA peroxidase was added to each well and incubated for 90 min. The plate was washed again and 2,29-azino-di-3-ethylbenzthiazoline sulfonate was added for color development. The amount of cytoplasmic DNA fragments was represented as absorbance at 405 nm.

Statistical analysis. All data were expressed as means ± SE. Differences between the three study groups were compared with one-way ANOVA, followed by Student-Newman-Keuls test.

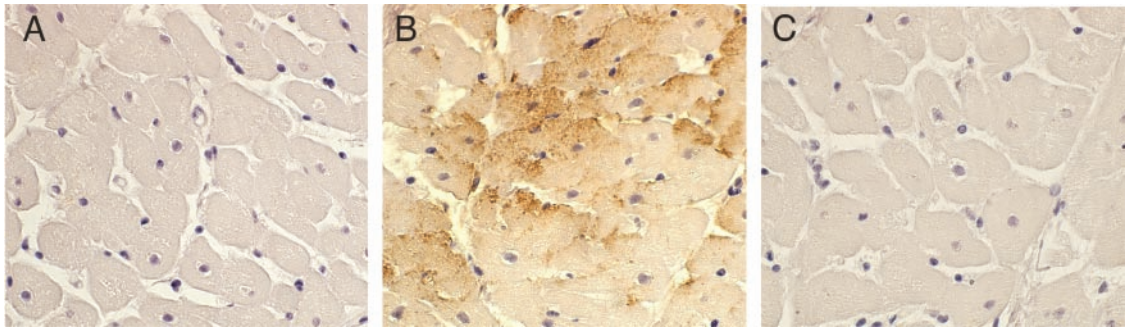

Fig. 1. TNF-α expression in the failing left ventricular (LV) myocardium (original magnification ×400). *A*: in the normal myocardium, TNF-α staining was negative. *B*: in the failing myocardium, TNF-α was expressed in cardiomyocytes. *C*: TNF-α negative control.

RESULTS

Effect of TNF-α inhibition on hemodynamics and LV remodeling. A representative example of immunohistochemical staining of TNF-α in the LV myocardium is shown in Fig. 1. TNF-α staining was negative in the normal control dogs. By contrast, in the untreated paced dogs, TNF-α was strongly expressed in cardiomyocytes. Consistent with increased myocardial TNF-α expression, plasma levels of TNF-α were also significantly increased in untreated paced dogs compared with normal control dogs (239 ± 92 vs. 10 ± 5 pg/ml; $P < 0.05$). Progression of CHF was assessed by hemodynamics and echocardiographic measures of LV performance and remodeling. Baseline hemodynamic and echocardiographic data were comparable in the three study groups (data not shown). As shown in Table 1, compared with the control group, chronic pacing resulted in marked increases in right and left-sided filling pressures, accompanied by decreases in mean arterial pressure, cardiac output, and LV peak positive developed pressure over time in the vehicle-treated group (paced vehicle). These severe hemodynamic perturbations were attenuated partially by in vivo inhibition of TNF-α in the etanercept-treated group (paced etanercept). As shown in Fig. 2, chronic pacing significantly reduced LV ejection fraction, increased LV end-diastolic volume, reduced LV mean wall thickness, and increased the diameter-to-length ratio (an index of globularity), changes that were consistent with marked LV chamber remodeling and impaired systolic performance. Chronic pacing with concomitant inhibition of TNF-α partially but significantly improved LV ejection fraction and reduced LV end-diastolic volume. The differences in LV mean wall thickness and diameter-to-length ratio between the vehicle-treated and the etanercept-treated dogs, however, did not reach statistical significance ($P = 0.271$ and $P = 0.276$, respectively).

Table 1. *Hemodynamic variables*

	Control	Paced Vehicle	Paced Etanercept
Body weight at baseline, kg	24±3	27±5	26±4
Heart rate, beats/min	81±3	127±13*	107±17†‡
Right atrial pressure, mmHg	5.6±0.5	15.5±1.6*	12.4±2.1†
LV end-diastolic pressure, mmHg	10±0	40±4*	31±5†‡
Mean arterial pressure, mmHg	107±3	93±9*	104±7‡
LV +dP/d*t*, mmHg/s	2,105±76	1,251±145*	1,626±261†‡
Cardiac output, 1/min	4.1±0.2	2.1±0.2*	2.9±0.4†‡

Values are means ± SE; $n = 10$ dogs per group. LV, left ventricular; +dP/d*t*, peak positive developed pressure over time; control, normal dogs; paced vehicle, vehicle-treated paced dogs; paced etancercept, etanercept-treated paced dogs. Data in the paced dogs were acquired with the pacing terminated. *$P < 0.01$, †$P < 0.05$ vs. control; ‡$P < 0.05$ vs. paced vehicle.

Effects of TNF-α inhibition on mitochondrial function. Specific activity levels of mitochondrial enzymes as well as the ratio of the activity of specific enzyme to CS are shown in Table 2. Myocardial complex V activity as well as complex V/CS activity ratio was significantly lower in the vehicle-treated paced animals. The level was restored in the etanercept-treated animals to level similar to those of the nonpaced control animals. Complex III activity and complex III/CS activity ratio were also significantly reduced in the vehicle-treated dogs, but unlike complex V was only partially restored in the etanercept-treated dogs. Levels of other mitochondrial enzyme activities, including respiratory complexes I, II, and IV, as well as CS, and activity ratios, were similar in the three groups. The activities of complexes III and V were also selectively reduced in the skeletal muscle of the vehicle-treated animals, but in contrast to the observation in the myocardium, the depressed enzyme activities were not altered by treatment with etanercept (Table 3).

Effect of TNF-α inhibition on oxidative stress. Myocardial oxidative stress was assessed by LV tissue aldehyde levels. A column of aldehydes and the sum total are shown in Table 4. Total aldehyde level in the LV was markedly increased in the vehicle-treated paced dogs. This increase in aldehyde level induced by pacing was driven mostly by the increase in unsaturated aldehyde species and malondialdehyde. TNF-α inhibition in the etanercept-treated dogs reduced these increased aldehyde levels to levels similar to those of the control nonpaced dogs.

Effect of TNF-α inhibition on myocyte apoptosis. Myocardial apoptosis was assessed by two independent methods: TUNEL assay and the photometric enzyme immunoassay for cytoplasmic histone-associated DNA fragments (cell death detection ELISA). An example of TUNEL assay is shown in Fig. 3. Chronic pacing significantly increased apoptosis as measured by the percentage of TUNEL-positive nuclei in the vehicle-treated paced dogs (Fig. 4*A*). Apoptosis was reduced significantly by TNF-α inhibition in the etanercept-treated dogs ($P < 0.05$). The results of the TUNEL staining were confirmed by the findings from cell death ELISA that measured cytoplasmic histone-associated DNA fragments (Fig. 4*B*).

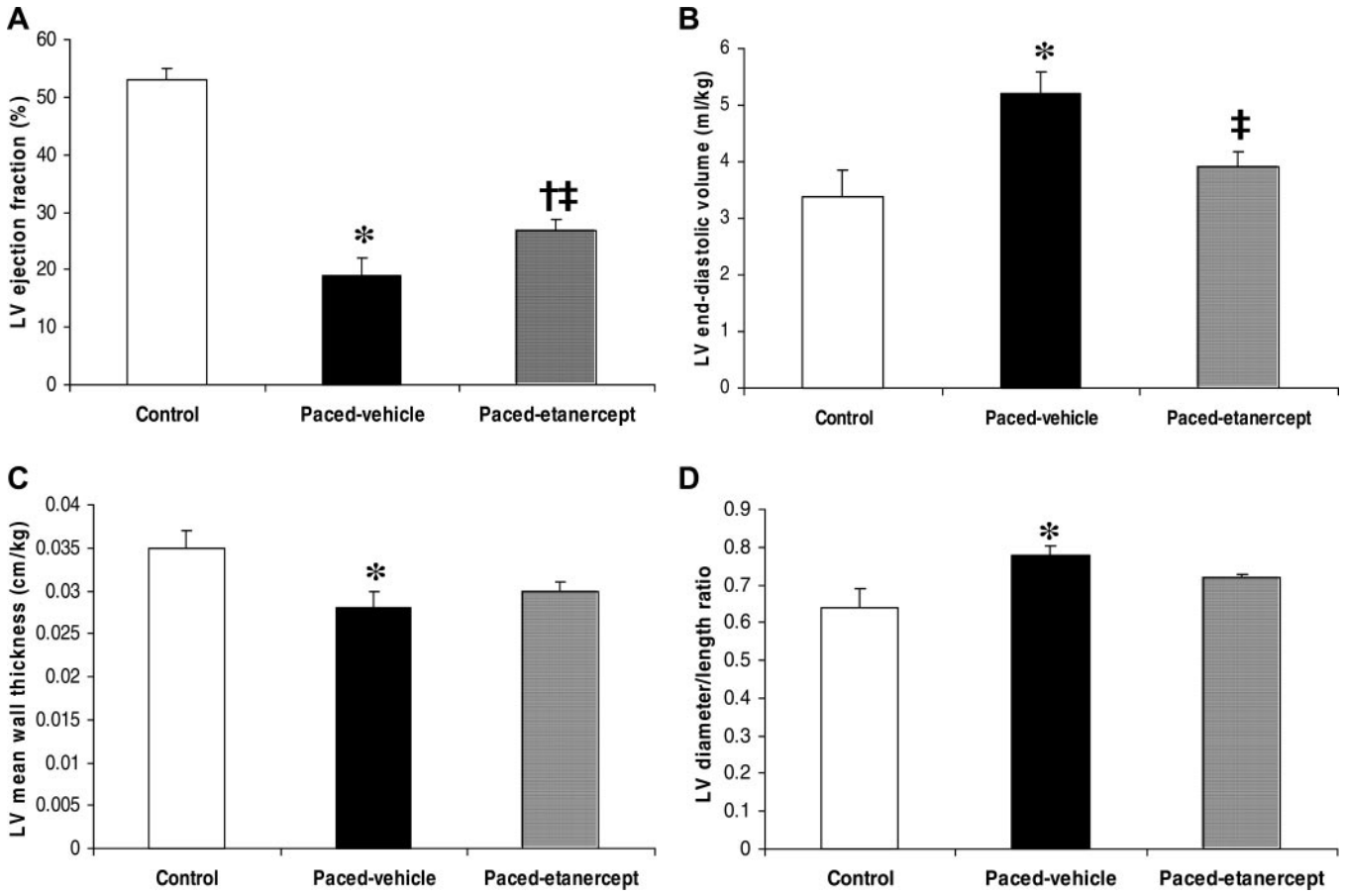

Fig. 2. Effects of chronic pacing and in vivo inhibition of TNF-α on echocardiographic measures of LV remodeling and function. *A*: LV ejection fraction; *B*: LV end-diastolic volume; *C*: LV mean wall thickness; and *D*: LV diameter-to-length ratio. Control, normal dogs; paced vehicle, vehicle-treated paced dogs; and paced etanercept, etanercept-treated paced dogs. *$P < 0.01$, †$P < 0.05$ vs. control; ‡$P < 0.05$ vs. vehicle-treated paced dogs.

DISCUSSION

Activation of the proinflammatory cytokines has been implicated in contributing to the progression of LV remodeling and pump dysfunction in both experimental and clinical settings of CHF (2, 9, 13, 20, 21). With the use of ELISA, we have previously demonstrated in canine pacing-induced CHF a marked increase in immuoreactive TNF-α level in both the serum and the LV myocardium (27, 28, 32). In the present study, the activation of TNF-α was confirmed with myocardial immunohistochemical staining and measurement of plasma TNF-α levels. However, up until now, the mechanisms linking the activation of TNF-α and progression of CHF remain unclear. The present study examined the effects of in vivo inhibition of TNF-α on LV remodeling and hemodynamic progression of CHF and concurrently measured myocardial mitochondrial function, oxidative stress, and apoptosis, in a unique CHF canine model of dilated cardiomyopathy. Our

Table 2. *Mitochondrial cardiac enzyme activities and activity ratios*

	Control	Paced Vehicle	Paced Etanercept
Complex I	52±6	46±7	41±7
Complex I/CS	0.060±0.006	0.052±0.006	0.070±0.010
Complex II	31±5	29±6	40±4
Complex II/CS	0.060±0.002	0.050±0.006	0.080±0.010
Complex III	8.8±0.8	1.7±0.6*	3.5±0.4†‡
Complex III/CS	0.012±0.002	0.004±0.001*	0.007±0.001†‡
Complex IV/CS	0.35±0.03	0.32±0.03	0.36±0.02
Complex V	163±20	51±6*	150±28‡
Complex V/CS	0.29±0.09	0.08±0.03*	0.23±0.1‡
Citrate synthase	533±36	546±40	528±46

Values are means ± SE; $n = 10$ dogs per group. CS, citrate synthase. All enzymes units are expressed as micromoles substrate used per minute per milligram of protein. *$P < 0.01$, †$P < 0.05$ vs. control, ‡$P < 0.05$ vs. paced vehicle.

Table 3. *Mitochondrial skeletal muscle enzyme activities and activity ratios*

	Control	Paced Vehicle	Paced Etanercept
Complex III	10.5±1.5	0.9±0.4*	1.6±0.5*
Complex III/CS	0.04±0.01	0.004±0.002*	0.006±0.003*
Complex IV	143±7	138.1±14.4	141±8.9
Complex IV/CS	0.50±0.05	0.51±0.06	0.48±0.07
Complex V	151±14	84±5*	107±4†
Complex V/CS	0.51±0.05	0.31±0.03*	0.38±0.06*
Citrate synthase	315±38	287±27	252±32

Values are means ± SE; $n = 4$ dogs per group. All enzymes units are expressed as micromoles substrate per minute per milligram of protein. *$P < 0.05$, †$P < 0.05$ vs. control.

Table 4. *LV tissue aldehyde levels*

Aldehydes	Control (n = 10)	Paced Vehicle (n = 9)	Paced Etanercept (n = 9)
Saturated			
Octanal	188±23	82±5*	91±6*
Nonanal	605±21	423±17†	418±22†
Unsaturated			
t-2-Heptenal	2,493±216	2,087±256	2,269±245
t-2-Octenal	126±6	112±7	112±8
t-2-Nonenal	93±4	146±14*	101±9†‡
4-OH-Hexenal	1,322±97	2,020±30*	1,572±54‡
4-OH-Nonenal	758±78	824±74*	740±35‡
4-OH-Decenal	6.6±0.3	4.8±0.3	5.1±0.3
t-2,*c*-6-Nonadienal	4.2±0.6	10.0±0.7*	5.6±0.4‡
t-2,*t*-4-Nonadienal	186±9	249±31*	203±19†‡
Malondialdehyde	1,266±122	5,804±1,306*	1,473±271‡
Total	7,048±448	11,760±1,410*	6,991±516‡

Values are means ± SE; n, no. or animals per group. *$P < 0.01$, †$P < 0.05$ vs. control; ‡$P < 0.05$ vs. paced vehicle.

findings are novel in two respects. First, together with our previous report (4) on the effects of etanercept on extracellular matrix remodeling, our studies represent the only preclinical studies of anti-TNF-α therapy in CHF. Second, to our knowledge, the current study is the first to examine in vivo the relationships among TNF-α, mitochondrial dysfunction, oxidative stress and apoptosis in pacing-induced CHF. Our principal findings are as follows. First, inhibition of TNF-α attenuated LV remodeling and hemodynamic deterioration induced by chronic pacing and significantly improved LV systolic function. Second, chronic pacing induced severe myocardial mitochondrial dysfunction, oxidative stress, and apoptosis, which were fully or partially reversed by concomitant TNF-α inhibition.

Mitochondrial function. Mitochondrial dysfunction may play an important pathogenetic role in the progression of CHF. In support of this hypothesis are numerous observations of reduced mitochondrial bioenergetic function in both experimental and clinical settings of CHF (27). In a previous study (26), using the canine model of pacing-induced CHF, we reported markedly reduced LV tissues levels of specific mitochondrial enzyme activities for respiratory complex III and complex V, an enzyme that was critical to the generation of ATP. Furthermore, the reduced myocardial complex III and complex V levels correlated with the increased LV tissue TNF-α protein levels, suggesting an association between increased TNF-α and mitochondrial dysfunction. On the other hand, a previous study in patients with CHF had reported reduced complex I but not complexes II, III, and IV, activities (37). However, interpretation of their data is confounded by the fact that their data were not normalized to substrate. Indeed, in vitro studies have suggested that the mitochondria appear to constitute a critical target of several of the actions that TNF-α exerts on cardiomyocytes, which may adversely affect cardiac function. For example, TNF-α can inhibit mitochondrial function directly through downregulation of respiratory chain activities (45) or induce mitochondrial damage and reduce respiratory chain complex III activity indirectly through an increase in oxygen free radicals (40). On the other hand, increased oxidative stress may in turn be a by-product of TNF-α induced mitochondrial dysfunction (38). Our present findings that the reduced myocardial complex III and complex V activities were reversed partially or completely by TNF-α inhibition therefore provided evidence to suggest that TNF-α contributed to the progression of LV remodeling and CHF, in part, through the induction of myocardial mitochondrial dysfunction. Interestingly, the levels of skeletal muscle mitochondrial complex III and V activities, which were reduced significantly in the vehicle-treated dogs, were not affected by TNF-α inhibition. Because etanercept was administered systemically, the cardiac-specific restoration of complex III and complex V activities by etanercept suggests that TNF-α induces mitochondrial dysfunction to a greater extent in the failing heart than in the skeletal muscle. In contrast, our previous experiments, which examined the effect of selective type A endothelin receptor blockade in pacing-induced CHF, demonstrated reversal of specific mitochondrial enzymatic deficiency in both the cardiac and skeletal muscle (28). This finding raises the possibility that TNF-α exerts more cardiac-specific effects on mitochondrial function during evolving CHF.

Oxidative stress. Our observation of markedly increased LV tissue levels of aldehydes in the vehicle-treated paced animal is relevant not only as an indication of increased oxidative stress, but also because of the potential of adverse effects from increased aldehydes, particularly those of the unsaturated al-

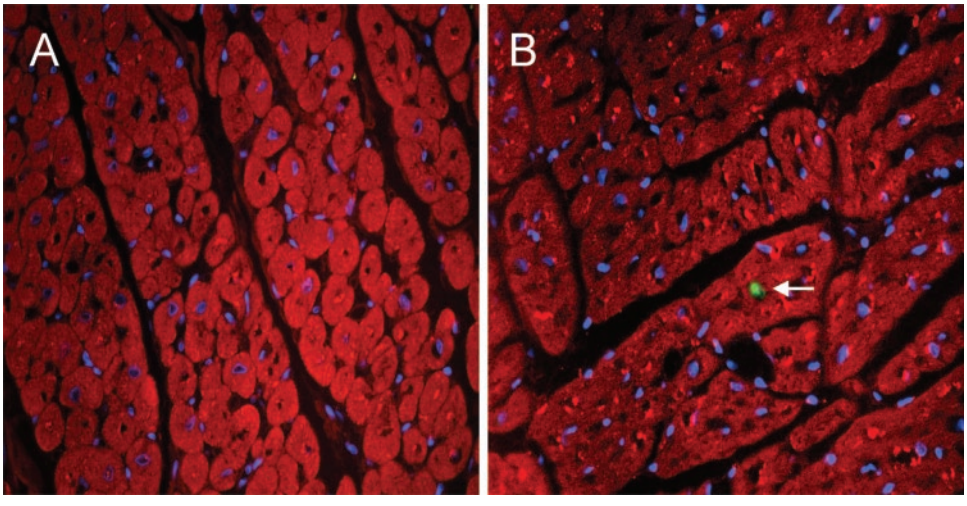

Fig. 3. Terminal deoxynucleotidyl transferase-mediated nick-end labeling (TUNEL) and cardiac troponin-I double staining (original magnification ×200). *A*: negative TUNEL staining from a control dog. *B*: TUNEL-positive cardiomyocyte nucleus is shown in green (arrow) from a paced dog. Cardiac troponin I staining is in red and nuclei are stained in blue by Hoechst 33258.

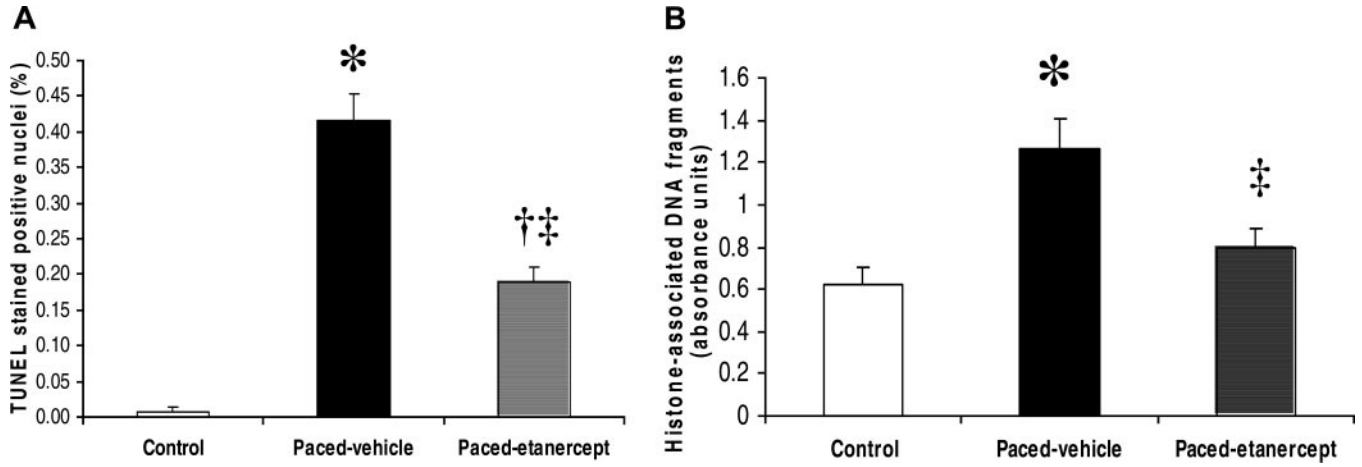

Fig. 4. Effects of chronic pacing and in vivo inhibition of TNF-α on apoptosis as measured by TUNEL staining (*A*) and cell death-detection ELISA (*B*). *$P < 0.01$; †$P < 0.05$ vs. control; ‡$P < 0.05$ vs. vehicle-treated paced dogs.

dehydes, on cardiac function (10, 11, 23). TNF-α can generate free radicals in the myocardium through a variety of mechanisms (15, 24). As mentioned earlier, increased oxidative stress can induce mitochondrial dysfunction, or in turn, result from mitochondrial dysfunction or damage (38, 40). Our present findings that upstream in vivo inhibition of TNF-α normalized LV tissue aldehyde levels provided evidence that TNF-α contributed to the progression of CHF in part via an increase in oxidative stress. Furthermore, the complex and partly bidirectional relationships among TNF-α receptor activation, increased oxidative stress, and mitochondrial dysfunction may amplify the detrimental effect of each of these pathological mechanisms on cardiac function (14, 38, 40, 45).

Apoptosis. Myocyte apoptosis has been observed in the myocardium in heart failure. Although the number of apoptotic myocytes is low at any given time point in heart failure, the accumulated number from apoptotic cell loss over time may be high enough to cause myocardial dysfunction (34). In this regard, we (32) recently demonstrated that the accumulated apoptotic cell death correlates significantly with myocardial dysfunction in pacing-induced heart failure. Consistent with this notion, a recent study (43) has also demonstrated a causal relationship between ongoing low levels of cardiomyocyte apoptosis and development of heart failure using cardiac-specific overexpression of caspase-8 in mice.

TNF-α can activate caspase and therefore trigger apoptosis through a multitude of molecular mechanisms (17). These mechanisms include the death receptor pathway that involves death domain-mediated protein-protein interactions, as well as the mitochondrial pathway that involves the release of cytochrome *c* (7, 17). In the cardiomyocytes, TNF-α-induced apoptosis appears to involve the sphingolipid-ceramide pathways with generation of the second messengers ceramide and sphingosine (19). Ceramide also inhibits mitochondrial respiratory chain complex III (35) and increases cytochrome *b* (16), which in turn results in activation of caspases and the triggering of apoptosis. Furthermore, oxidative stress upregulates TNF-α and induces cardiomyocyte apoptosis and both were decreased by pretreatment with anti-TNF-α antibodies, suggesting that oxidative stress induces apoptosis of cardiomyocytes partly through TNF-α (1). Our current findings that TNF-α inhibition significantly reduced myocardial apoptosis in the etanercept-treated paced dogs provided evidence that the pro-apoptotic effect of TNF-α contributes to the progression of CHF.

Physiological relevance and potential limitations. Findings from our study provide evidence that activated TNF-α contributes to LV remodeling and dysfunction and to the progression of CHF through the local induction of mitochondrial dysfunction, oxidative stress, and apoptosis. One important finding of our study is that except for LV tissue mitochondrial respiratory enzyme complex V activity and aldehyde levels, etanercept was unable to fully restore other study parameters, including indexes of LV remodeling and systolic function, hemodynamics, and measurements of apoptosis to control values. Furthermore, the lower heart rate in the treated animals may have accounted in part for the improved ejection fraction in the treated dogs. The lack of a complete restoration of cardiac function, however, was not entirely unexpected because TNF-α and cytokine activation is unlikely to be the sole mechanism mediating CHF progression. Neurohormonal mechanisms, which play a key role in mediating the progression of CHF and are markedly activated in this canine model of CHF (30), were not pharmacologically inhibited in our current study. It should be emphasized again that the principal aim of our study was to use etanercept as a probe to examine mechanistically the pathophysiological role of TNF-α and not to describe the clinical utility of etanercept. Our findings therefore provide one of several explanations for the failure to demonstrate therapeutic benefits of etanercept, a chimeric monoclonal antibody to soluble TNF-α receptor, on patients with CHF (6, 22). In these clinical trials of TNF-α inhibition, patients were at various stage of disease progression: many of them had co-morbid conditions, such as hypertension and diabetes, and were already on optimized therapy for heart failure, including neurohormonal inhibition. This renders the demonstration of incremental benefit from additional therapeutic approaches, particularly in a short time frame, extremely difficult, and may lead to erroneous conclusion that cytokine activation does not play a pathogenic role in evolving CHF. This highlights the importance of the use of intact animal models to study in vivo regulatory mechanisms, instead of

relying solely on the results of clinical trials. On the other hand, one limitation of intact animal studies is that it is impossible to finely resolve the contribution of each cellular event and temporal order, although one can conclude with reasonable certainty on the net effect of the interplay of different cellular mechanisms.

In summary, the present study demonstrated an important role of TNF-α in the progression of heart failure in a pacing dog model. Increased TNF-α contributes to progressive LV dysfunction, mediated in part by a local impairment in mitochondrial function and increase in oxidative stress and myocyte apoptosis.

GRANTS

This study was supported by the Heart and Stroke Foundation of Ontario Grants-in-Aid T-4782 (to G. W. Moe) and T-4923 (to Q. Feng). Q. Feng was a recipient of a Research Career Award from Rx&D Health Research Foundation and Canadian Institutes of Health Research.

REFERENCES

1. **Aikawa R, Nitta-Komatsubara Y, Kudoh S, Takano H, Nagai T, Yazaki Y, Nagai R, and Komuro I.** Reactive oxygen species induce cardiomyocyte apoptosis partly through TNF-alpha. *Cytokine* 18: 179–183, 2002.
2. **Bozkurt B, Kribbs SB, Clubb FJ Jr, Michael LH, Didenko VV, Hornsby PJ, Seta Y, Oral H, Spinale FG, and Mann DL.** Pathophysiologically relevant concentrations of tumor necrosis factor-alpha promote progressive left ventricular dysfunction and remodeling in rats. *Circulation* 97: 1382–1391, 1998.
3. **Bradford MM.** A rapid and sensitive method for the quantitation of microgram quantities of protein utilizing the principle of protein-dye binding. *Anal Biochem* 72: 248–254, 1976.
4. **Bradham WS, Moe G, Wendt KA, Scott AA, Konig A, Romanova M, Naik G, and Spinale FG.** TNF-α and myocardial matrix metalloproteinases in heart failure: relationship to LV remodeling. *Am J Physiol Heart Circ Physiol* 282: H1288–H1295, 2002.
5. **Byrne JA, Grieve DJ, Cave AC, and Shah AM.** Oxidative stress and heart failure. *Arch Mal Coeur Vaiss* 96: 214–221, 2003.
6. **Chung ES, Packer M, Lo KH, Fasanmade AA, and Willerson JT.** Randomized, double-blind, placebo-controlled, pilot trial of infliximab, a chimeric monoclonal antibody to tumor necrosis factor-alpha, in patients with moderate-to-severe heart failure: results of the anti-TNF Therapy Against Congestive Heart Failure (ATTACH) trial. *Circulation* 107: 3133–3140, 2003.
7. **Cohen GM.** Caspases: the executioners of apoptosis. *Biochem J* 326: 1–16, 1997.
8. **Cohn JN, Ferrari R, and Sharpe N.** Cardiac remodeling–concepts and clinical implications: a consensus paper from an international forum on cardiac remodeling. Behalf of an International Forum on Cardiac Remodeling. *J Am Coll Cardiol* 35: 569–582, 2000.
9. **Deswal A, Bozkurt B, Seta Y, Parilti-Eiswirth S, Hayes FA, Blosch C, and Mann DL.** Safety and efficacy of a soluble P75 tumor necrosis factor receptor (Enbrel, etanercept) in patients with advanced heart failure. *Circulation* 99: 3224–3226, 1999.
10. **Eaton P, Li JM, Hearse DJ, and Shattock MJ.** Formation of 4-hydroxy-2-nonenal-modified proteins in ischemic rat heart. *Am J Physiol Heart Circ Physiol* 276: H935–H943, 1999.
11. **Edes I, Toszegi A, Csanady M, and Bozoky B.** Myocardial lipid peroxidation in rats after chronic alcohol ingestion and the effects of different antioxidants. *Cardiovasc Res* 20: 542–548, 1986.
12. **Esterbauer H and Zollner H.** Methods for determination of aldehydic lipid peroxidation products. *Free Radic Biol Med* 7: 197–203, 1989.
13. **Feldman AM, Combes A, Wagner D, Kadakomi T, Kubota T, Li YY, and McTiernan C.** The role of tumor necrosis factor in the pathophysiology of heart failure. *J Am Coll Cardiol* 35: 537–544, 2000.
14. **Feng L, Xia Y, Garcia GE, Hwang D, and Wilson CB.** Involvement of reactive oxygen intermediates in cyclooxygenase-2 expression induced by interleukin-1, tumor necrosis factor-alpha, and lipopolysaccharide. *J Clin Invest* 95: 1669–1675, 1995.
15. **Feng L, Xia Y, Garcia GE, Hwang D, and Wilson CB.** Involvement of reactive oxygen intermediates in cyclooxygenase-2 expression induced by interleukin-1, tumor necrosis factor-alpha, and lipopolysaccharide. *J Clin Invest* 95: 1669–1675, 1995.
16. **Gudz TI, Tserng KY, and Hoppel CL.** Direct inhibition of mitochondrial respiratory chain complex III by cell-permeable ceramide. *J Biol Chem* 272: 24154–24158, 1997.
17. **Haunstetter A and Izumo S.** Apoptosis: basic mechanisms and implications for cardiovascular disease. *Circ Res* 82: 1111–1129, 1998.
18. **Howard RJ, Moe GW, and Armstrong PW.** Sequential echocardiographic-Doppler assessment of left ventricular remodelling and mitral regurgitation during evolving experimental heart failure. *Cardiovasc Res* 25: 468–474, 1991.
19. **Krown KA, Page MT, Nguyen C, Zechner D, Gutierrez V, Comstock KL, Glembotski CC, Quintana PJ, and Sabbadini RA.** Tumor necrosis factor alpha-induced apoptosis in cardiac myocytes. Involvement of the sphingolipid signaling cascade in cardiac cell death. *J Clin Invest* 98: 2854–2865, 1996.
20. **Kubota T, McTiernan CF, Frye CS, Slawson SE, Lemster BH, Koretsky AP, Demetris AJ, and Feldman AM.** Dilated cardiomyopathy in transgenic mice with cardiac-specific overexpression of tumor necrosis factor-alpha. *Circ Res* 81: 627–635, 1997.
21. **Lisman KA, Stetson SJ, Koerner MM, Farmer JA, and Torre-Amione G.** The role of inflammation in the pathogenesis of heart failure. *Curr Cardiol Rep* 4: 200–205, 2002.
22. **Louis A, Cleland JG, Crabbe S, Ford S, Thackray S, Houghton T, and Clark A.** Clinical trials update: CAPRICORN, COPERNICUS, MIRACLE, STAF, RITZ-2, RECOVER and RENAISSANCE and cachexia and cholesterol in heart failure. Highlights of the Scientific Sessions of the American College of Cardiology, 2001. *Eur J Heart Fail* 3: 381–387, 2001.
23. **Luo XP, Yazdanpanah M, Bhooi N, and Lehotay DC.** Determination of aldehydes and other lipid peroxidation products in biological samples by gas chromatography-mass spectrometry. *Anal Biochem* 228: 294–298, 1995.
24. **Machida Y, Kubota T, Kawamura N, Funakoshi H, Ide T, Utsumi H, Li YY, Feldman AM, Tsutsui H, Shimokawa H, and Takeshita A.** Overexpression of tumor necrosis factor-α increases production of hydroxyl radical in murine myocardium. *Am J Physiol Heart Circ Physiol* 284: H449–H455, 2003.
25. **Mak S, Lehotay DC, Yazdanpanah M, Azevedo ER, Liu PP, and Newton GE.** Unsaturated aldehydes including 4-OH-nonenal are elevated in patients with congestive heart failure. *J Card Fail* 6: 108–114, 2000.
26. **Marin-Garcia J, Goldenthal MJ, and Moe GW.** Abnormal cardiac and skeletal muscle mitochondrial function in pacing-induced cardiac failure. *Cardiovasc Res* 52: 103–110, 2001.
27. **Marin-Garcia J, Goldenthal MJ, and Moe GW.** Mitochondrial pathology in cardiac failure. *Cardiovasc Res* 49: 17–26, 2001.
28. **Marin-Garcia J, Goldenthal MJ, and Moe GW.** Selective endothelin receptor blockade reverses mitochondrial dysfunction in canine heart failure. *J Card Fail* 8: 326–332, 2002.
29. **Meldrum DR.** Tumor necrosis factor in the heart. *Am J Physiol Regul Integr Comp Physiol* 274: R577–R595, 1998.
30. **Moe GW and Armstrong P.** Pacing-induced heart failure: a model to study the mechanism of disease progression and novel therapy in heart failure. *Cardiovasc Res* 42: 591–599, 1999.
31. **Moe GW, Grima EA, Wong NL, Howard RJ, and Armstrong PW.** Plasma and cardiac tissue atrial and brain natriuretic peptides in experimental heart failure. *J Am Coll Cardiol* 27: 720–727, 1996.
32. **Moe GW, Naik G, Konig A, Lu X, and Feng Q.** Early and persistent activation of myocardial apoptosis, bax and caspases: insights into mechanisms of progression of heart failure. *Pathophysiology* 8: 183–192, 2002.
33. **Nakamura K, Fushimi K, Kouchi H, Mihara K, Miyazaki M, Ohe T, and Namba M.** Inhibitory effects of antioxidants on neonatal rat cardiac myocyte hypertrophy induced by tumor necrosis factor-alpha and angiotensin II. *Circulation* 98: 794–799, 1998.
34. **Sabbah HN.** Apoptotic cell death in heart failure. *Cardiovasc Res* 45: 704–712, 2000.
35. **Sanchez-Alcazar JA, Schneider E, Martinez MA, Carmona P, Hernandez-Munoz I, Siles E, De La TP, Ruiz-Cabello J, Garcia I, and Solis-Herruzo JA.** Tumor necrosis factor-alpha increases the steady-state reduction of cytochrome b of the mitochondrial respiratory chain in metabolically inhibited L929 cells. *J Biol Chem* 275: 13353–13361, 2000.
36. **Satoh M, Nakamura M, Saitoh H, Satoh H, Maesawa C, Segawa I, Tashiro A, and Hiramori K.** Tumor necrosis factor-alpha-converting

enzyme and tumor necrosis factor-alpha in human dilated cardiomyopathy. *Circulation* 99: 3260–3265, 1999.

37. **Scheubel RJ, Tostlebe M, Simm A, Rohrbach S, Prondzinsky R, Gellerich FN, Silber RE, and Holtz J.** Dysfunction of mitochondrial respiratory chain complex I in human failing myocardium is not due to disturbed mitochondrial gene expression. *J Am Coll Cardiol* 40: 2174–2181, 2002.
38. **Schulze-Osthoff K, Bakker AC, Vanhaesebroeck B, Beyaert R, Jacob WA, and Fiers W.** Cytotoxic activity of tumor necrosis factor is mediated by early damage of mitochondrial functions. Evidence for the involvement of mitochondrial radical generation. *J Biol Chem* 267: 5317–5323, 1992.
39. **Song W, Lu X, and Feng Q.** Tumor necrosis factor-alpha induces apoptosis via inducible nitric oxide synthase in neonatal mouse cardiomyocytes. *Cardiovasc Res* 45: 595–602, 2000.
40. **Suematsu N, Tsutsui H, Wen J, Kang D, Ikeuchi M, Ide T, Hayashidani S, Shiomi T, Kubota T, Hamasaki N, and Takeshita A.** Oxidative stress mediates tumor necrosis factor-alpha-induced mitochondrial DNA damage and dysfunction in cardiac myocytes. *Circulation* 107: 1418–1423, 2003.
41. **Van der PT, Coyle SM, Levi M, Jansen PM, Dentener M, Barbosa K, Buurman WA, Hack CE, ten Cate JW, Agosti JM, and Lowry SF.** Effect of a recombinant dimeric tumor necrosis factor receptor on inflammatory responses to intravenous endotoxin in normal humans. *Blood* 89: 3727–3734, 1997.
42. **Weinblatt ME, Kremer JM, Bankhurst AD, Bulpitt KJ, Fleischmann RM, Fox RI, Jackson CG, Lange M, and Burge DJ.** A trial of etanercept, a recombinant tumor necrosis factor receptor:Fc fusion protein, in patients with rheumatoid arthritis receiving methotrexate. *N Engl J Med* 340: 253–259, 1999.
43. **Wencker D, Chandra M, Nguyen K, Miao W, Garantziotis S, Factor SM, Shirani J, Armstrong RC, and Kitsis RN.** A mechanistic role for cardiac myocyte apoptosis in heart failure. *J Clin Invest* 111: 1497–1504, 2003.
44. **Wyatt HL, Heng MK, Meerbaum S, Hestenes JD, Cobo JM, Davidson RM, and Corday E.** Cross-sectional echocardiography. I. Analysis of mathematic models for quantifying mass of the left ventricle in dogs. *Circulation* 60: 1104–1113, 1979.
45. **Zell R, Geck P, Werdan K, and Boekstegers P.** TNF-alpha and IL-1 alpha inhibit both pyruvate dehydrogenase activity and mitochondrial function in cardiomyocytes: evidence for primary impairment of mitochondrial function. *Mol Cell Biochem* 177: 61–67, 1997.